Electronic Research Archive

ERA, 31(12): 7224–7243.
DOI: 10.3934/era.2023366
Received: 20 November 2022
Revised: 16 October 2023
Accepted: 22 October 2023
Published: 13 November 2023

http://www.aimspress.com/journal/era

Research article

Compatibility investigation of waste plastics in bitumen via a molecular dynamics method

Hui Yao[1,*], Xin Li[1], Hancheng Dan[2], Qingli Dai[3] and Zhanping You[3]

[1] Beijing Key Laboratory of Traffic Engineering, Faculty of Architecture, Civil and Transportation Engineering, Beijing University of Technology, No. 100, Pingleyuan, Chaoyang, Beijing 100124, China
[2] School of Civil Engineering, Central South University, Changsha, Hunan 410075, China; Rail Data Research and Application Key Laboratory of Hunan Province, Central South University, Changsha, Hunan 410075, China; Hunan Tieyuan Civil Engineering Testing Co., Ltd., Changsha, Hunan 410075, China
[3] Department of Civil and Environmental Engineering, Michigan Technological University, Houghton, MI 49931-1295, USA

* **Correspondence:** Email: huiyao@mtu.edu.

Abstract: The compatibility between waste plastic polymers and bitumen is the most challenging issue hindering the improvement of modified bitumen performance. The current practice of recycled waste plastics includes the use of polyvinyl chloride (PVC), polypropylene (PP), polyethylene (PE), etc. This study was designed to investigate the compatibility of different waste plastic polymers with bitumen binders by conducting molecular dynamics (MD) simulations at different temperatures. The molecular models of these materials were constructed in this study for the compatibility analysis, and they include the base bitumen, polymers (PVC, PP, and PE), polymer- bitumen blending systems. Using the output and related calculations of these MD models, the properties of these blending systems were measured at different temperatures through the calculation of the solubility parameter (δ) and interaction energies. The compatibility analysis is discussed in the context of these simulation results. The simulation results for the solubility parameters and interaction energies show consistent trends. The results showed that PVC and PP had better compatibility with bitumen at 433.15 K and that PE and bitumen had good compatibility at 393.15 K. Moreover, it can be deduced that the order of compatibility of the three polymers with bitumen is as follows: PVC > PE > PP. In addition, these research results can be referenced for the industry and research development of modified bitumen.

Keywords: pavement engineering; waste plastics; polyvinyl chloride; polypropylene; polyethylene; polymer modified bitumen; compatibility; molecular dynamics

1. Introduction

Currently, more and more material waste is being accumulated every day, while the issue of plastic waste is also being raised globally. According to the related report, total plastic consumption in Australia was 3,531,100 tons from 2016 to 2017 [1]. In recent years, more than 30 million tons of plastic waste materials have been found to be produced in China each year [2]. According to the data reported by the European Union (EU) and the USA, most of the plastic waste materials in the EU were processed via incineration, and only about 30% of plastic waste materials were recycled [3]. According to the data from the USA's Environmental Protection Agency, only 8.4% of plastic waste materials were recycled and 75.8% of waste materials were discarded in a landfill [4]. The landfills cause pollution problems for the lands and water, and waste plastics threaten the environment and public health [5]. Researchers are currently exploring different methods to reuse and recycle waste plastics.

Meanwhile, bitumen pavement is currently the main type of pavement in the world. Due to traffic loads, environmental factors, material aging and construction deficiencies, the early damage and deterioration of pavement are accelerated [6–8]. This situation has necessitated an improvement in the performance of the bitumen materials. Research has been conducted to find effective modifiers to improve pavement performance [9–12]. The addition of polymers is a typical modification process for bitumen materials [13]. Numerous studies have shown that polymer modifiers can improve the elasticity and ductility of modified bitumen effectively, as well as improve bitumen's crack resistance [14–16]. Plastic waste materials have been sorted and reprocessed in steps to produce single polymer particles, which were introduced into the bitumen as polymer modifiers to improve performance [17–20]. For the purpose of introducing polymer-modified bitumen to the road industry, researchers have applied most of the available polymers as bitumen modifiers [21,22]. According to Wu and Montalvo [23] and Vargas and El Hanandeh [24], the major types of waste polymers used for bitumen modification are as follows: polyethylene terephthalate (PET) [7,25,26], high-density polyethylene (HDPE) [27–29], polyvinyl chloride (PVC) [8,30,31], low-density polyethylene (LDPE) [28,32,33], polypropylene (PP) [33–35] and polystyrene [36–38]. Other polymers that are attracting researchers' attention are ethylene vinyl acetate [39–41] and polyurethane [6,42,43], acrylonitrile butadiene styrene [44–46]. However, the high market price of polymer modifiers has increased the cost of modified bitumen and pavement. The recycling of waste plastics effectively solves this problem. The most commonly recycled plastics are PVC, PP and polyethylene (PE). The research results show that PVC can increase the viscosity of the bitumen, as well as improve the leach resistance which minimizes permanent deformation, as well as crack resistance, and rutting resistance [8,47,48]. PP significantly enhanced the rutting resistance, fatigue resistance and crack resistance of modified bitumen [49]. PE enhanced the high-temperature stability of modified bitumen [50,51]. However, the properties of polymeric materials usually depend on their microstructure and synergistic effects, which are usually not directly accessible through macroscopic tests or other numerical methods.

The molecular dynamics (MD) method is one of the most powerful tools to understand the behavior of fluids and materials at the atomic level. The MD method simulates the molecular motion of particles at the atomic scale on the basis of classical and statistical mechanics. The paths and motion

of atoms and molecules are determined by Newton's laws, while the energy of molecules is determined by the force field. The MD method has historically played a key role in confirming the theory of fluid states [52]. Alder and Wainwright conducted the first MD simulation of a fluid and studied the macroscopic properties of substances for the first time [53]. Later, Rahman simulated the liquid water with the MD method [54]. In recent years, the MD simulations allowed direct evaluation of physical properties and were widely used in many natural science fields. The researchers found that MD has been applied to the field of road materials [55]. Khabaz and Khare studied the diffusion coefficient for bitumen as a function of temperature by conducting MD simulations [56].

The most important thing for an MD simulation of bitumen is to have an accurate model. Numerous scholars have done a lot of work on the molecular modeling of bitumen. Through the Strategic Highway Research Program (SHRP), Jennings proposed eight molecularly averaged structures of bitumen based on nuclear magnetic resonance techniques [57]. Pauli found that the surface energy and density of alicyclic sheet molecules with 13 rings were in the best agreement with the experimental results of SHRP bitumen samples obtained via the calculation of the density, refractive index, surface tension, etc. [58]. However, these models ignored some internal structures of bitumen because they did not consider interactive effects between components. Currently, the bitumen components are mainly divided into three-component and four-component systems. The three components include asphaltene, resin and oil. There are two mainstream methods for the analysis of the four components; one is based on the different solubilities of bitumen in different polar solvents and different adsorption capacities in the solid particle-packed column, and the bitumen can be divided into saturates, aromatics, resins and asphaltenes. The other one is the Corbett method which entailed using fractional distillation to divide bitumen into four components: asphaltene, polar aromatic, naphthene aromatic and saturate [59]. These two methods differ in the names of the components, but the principles are similar at the molecular level. Zhang and Greenfield divided bitumen into three components (resin, saturate and asphaltene) to investigate the density and isothermal compression properties of bitumen [60]. A simplified three-component bitumen model was proposed, where the n-docosane $(\mathrm{n}-C_{22}H_{46})$ and 1, 7-Dimethylnaphthalene were treated as saturates and aromatics and the asphaltene was selected as two molecules $C_{64}H_{52}S_2$ and $C_{72}H_{98}$S [61]. Subsequently, Li and Greenfield proposed a typical 12 models to represent the three-core bitumen for the SHRP binder, as shown in Figure 1; particularly, AAA-1, AAM-1 and AAK-1 were formed by the four components of the bitumen [62]. This model consists of larger molecules than the bitumen model proposed by Zhang and Greenfield, which improved the accuracy of the model through the corresponding density and thermal expansion coefficient. The four-component model proposed by Li and Greenfield is now widely used in bitumen molecular simulation studies. However, only the properties of AAA-1 bitumen represented by this model have been better validated and applied [62].

The compatibility is a property of the modifier particles that are uniformly distributed in the medium of bitumen without delamination or separation from each other [63]. There are significant differences between the structures and properties of bitumen and waste plastics, and the compatibility after blending is directly related to the structures and performance of the modified bitumen. Better performance can only be achieved when the bitumen and polymer are mutually compatible. There is growing concern about the compatibility between waste plastics and bitumen. Xin et al. reviewed and examined the distribution of PE in bitumen by using electron microscopy [64]. Rahman et al. studied the effect of PVC on bitumen and it was found that the ductility, permeability and solubility values for modified bitumen decreased with the increase in PVC content [65]. Tapkın proposed that PP enhanced

the rutting resistance, fatigue resistance and cracking resistance of modified bitumen [66]. Moreover, molecular simulation techniques have commonly been used to evaluate the compatibility between bitumen and polymers. Su et al. used MD simulations to study the compatibility between styrene-butadiene-styrene (SBS) and bitumen; they evaluated the miscibility of the two materials from the perspective of the solubility parameters. The results revealed that the miscibility of SBS and bitumen depends on the temperature range and van der Waals interactions play a dominant role in the miscibility of the bitumen/SBS system [67]. The compatibility of rubber and bitumen was also studied via MD simulation by using the solubility parameters and binding energy as indicators. The results revealed that, among the three main components of rubber (NR- natural rubber, BR- butadiene rubber, SBR- styrene butadiene rubber), BR is the most compatible with bitumen, SBR ranked the second and NR is the worst one [68]. The MD simulation was used to study the compatibility of PE with bitumen according to different resources. The compatibility of HDPE, medium-density PE, LDPE and linear low-density PE with bitumen was comparatively studied. It was found that LDPE had the best compatibility with bitumen compared to others [69]. In summary, it is feasible to study the compatibility of bitumen with polymers by using MD simulation techniques.

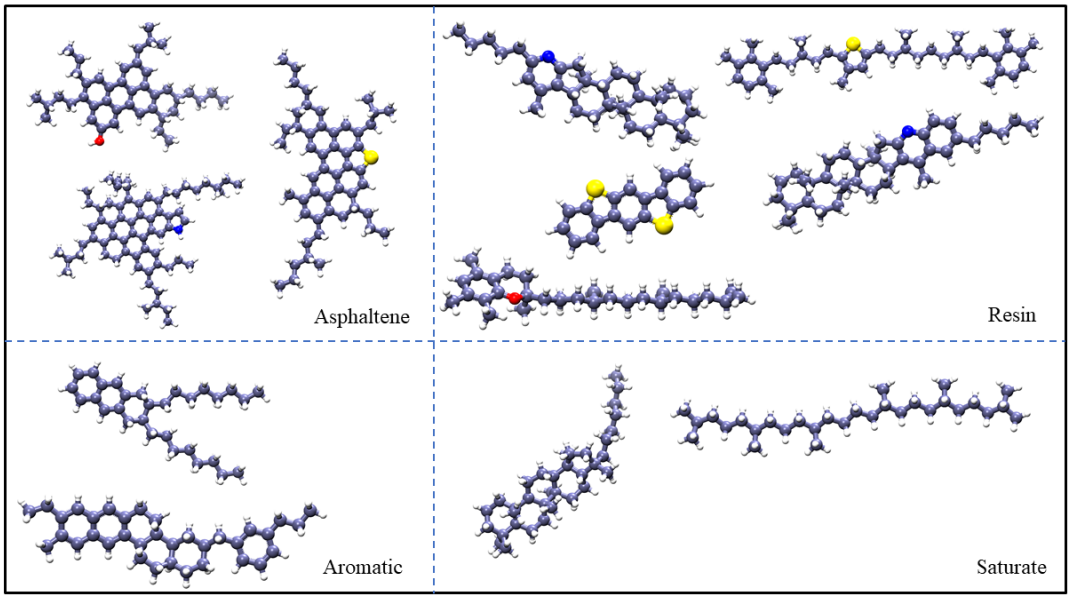

Figure 1. Representative molecules of bitumen components (the carbon atom is purple, the oxygen atom is red, the nitrogen atom is blue, the sulfur atom is yellow, and the hydrogen atom is white).

In this study, 12 molecular models proposed by Li and Greenfield were used to model the dynamics of bitumen molecules [62]. The model generation of polymers (PVC, PP and PE) was based on their molecular structures. The cohesive energy density (CED) and interaction energy of bitumen blending systems with polymers (PVC, PP, and PE) were calculated by using the MD simulation technique. The simulation results were analyzed to study the compatibility between waste polymers and bitumen. Figure 2 shows the flowchart of this study. The research results can be referenced for the waste polymers in pavement engineering.

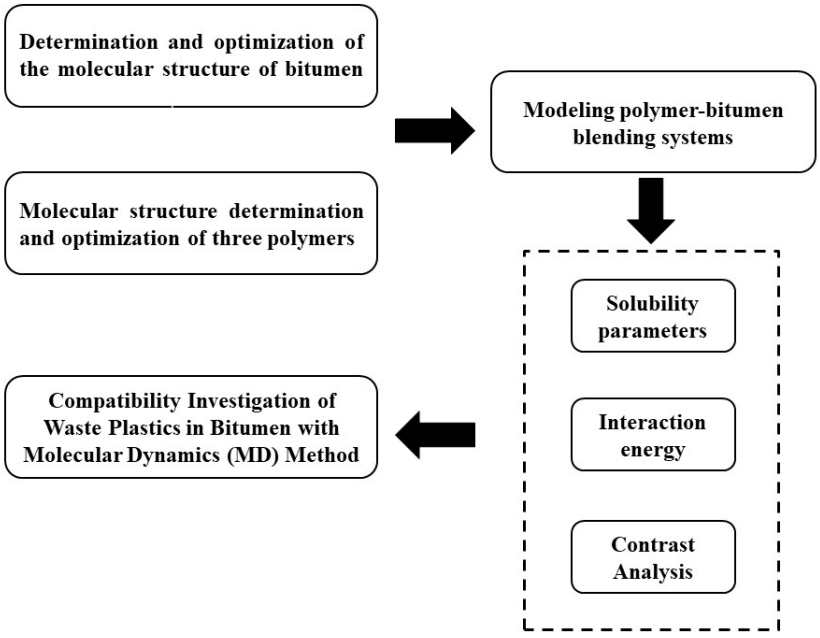

Figure 2. Flowchart of polymer and bitumen compatibility simulation.

2. Force field

The force field in MD simulations provides parameters for various types of atoms to calculate system energies in MD simulations. The basic and functional forms of energy include bonded and non-bonded terms in MD simulations. The AMBER Cornell extension force field (ACEFF) is derived from the Assisted Model Building with Energy Refinement (AMBER) programs [70]. The AMBER force field was originally used for the simulation of biological macromolecules, but researchers later added new parameters to this force field and derived the AMBER Cornell force field and general AMBER Force field, which were successfully used in the simulation of many biological organic molecules with good results [71]. The results have been successfully applied for the simulation of many bioorganic molecules with good results. The formula for the ACEFF is shown in Eq (1).

$$E_{total}=\sum_{bonds} K_r\left(\mathrm{r}-r_{eq}\right)^2+\sum_{angles} K_\theta\left(\theta-\theta_{eq}\right)^2+\sum_{dihedrals}\frac{V_n}{2}[1+\cos(n\varphi-\gamma)]+\sum_{i<j}\left[\frac{A_{ij}}{R_{ij}^{12}}-\frac{B_{ij}}{R_{ij}^{6}}+\frac{q_iq_j}{\in R_{ij}}\right] \tag{1}$$

where E_{total} means the total energy of the system, E_{bonds} means the energy of bonds, E_{angles} means the energy of angles, $E_{dihedrals}$ means the energy of dihedrals, and $E_{i<j}$ means non-bonded intersection energy. r_{eq} and θ_{eq} are the equilibrium structural parameters; K_r and K_θ are the force constants; n and γ are the multiplicity and phase angle for the torsional angle parameters, respectively; A, B and q are the non-bonded potentials between all atom pairs; finally, R is the distance corresponding to the calculation of non-bonded interactions; ϵ represents the van der Waals interaction corresponding to the trap depth.

3. Molecular models

3.1. Bitumen molecular models

Table 1. Molecular information of the 12-component bitumen model.

Component	Component	Chemical formula	Number of molecules
Asphaltene	Asphaltene-phenol	$C_{42}H_{54}O$	3
	Asphaltene-pyrrole	$C_{66}H_{81}N$	2
	Asphaltene-thiophene	$C_{51}H_{62}S$	3
Saturate	Squalane	$C_{30}H_{62}$	4
	Hopane	$C_{35}H_{62}$	4
Aromatic	DOCHN	$C_{30}H_{46}$	13
	PHPN	$C_{35}H_{44}$	11
	Quinolinohopane	$C_{40}H_{59}N$	4
	Benzobisbenzothiophene	$C_{18}H_{10}S_2$	15
Resin	Pyridinohopane	$C_{36}H_{57}N$	4
	Thioisorenieratane	$C_{40}H_{60}S$	4
	Trimethylbenzeneoxane	$C_{29}H_{50}O$	5

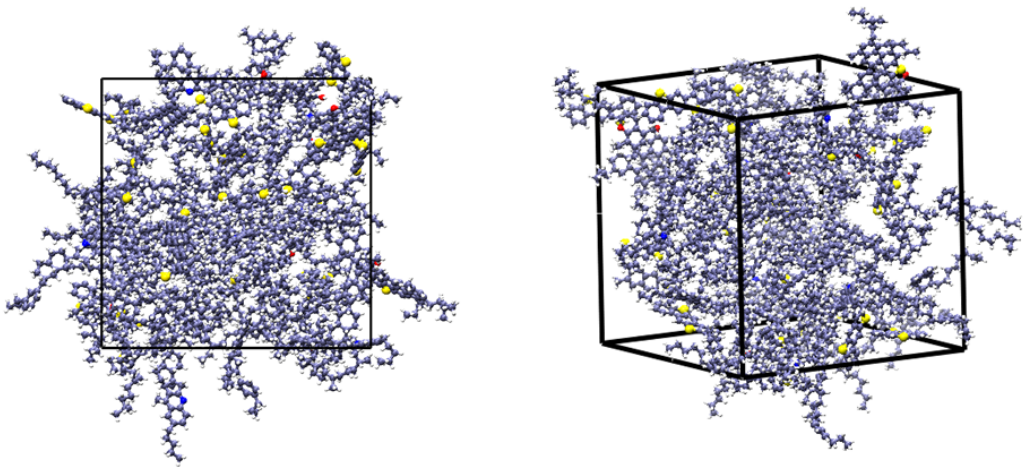

Figure 3. The basic bitumen molecular structures from different views, the left image from the top view and the right image from the side review (the carbon atom is purple, the oxygen atom is red, the nitrogen atom is blue, the sulfur atom is yellow, and the hydrogen atom is white).

In this study, the molecular composition in bitumen is shown in Table 1. The ACEFF [72] was used to model the bitumen molecules, as shown in Figure 3. Due to the high energy of the bitumen system, it may adversely affect the simulation calculations and it needs to be optimized to bring the bitumen to a stable equilibrium. The bitumen model with the ACEFF was equilibrated in three steps: 1) optimize the energy at the maximum 5000 iterations by using the conjugate gradient method; 2) subject it to 100 atm and 298.15 K for 200 ps (picosecond); 3) run for 1000 ps at 1 atm and 298.15 K [46,47]. The

minimum timestep of the simulation process is 1 fs, and the trajectory is recorded every 100 fs. It is common to use the density to validate the system in MD simulations; the variation pattern of the density with the number of iterations is shown in Figure 4(a). At the end of the simulation, the density was about 0.98 g/cm^3, which was close to the density of the real state, i.e., 0.95–1.15 g/cm^3. Figure 4(b) shows the change in energy of the bitumen during geometry optimization, which changes from 12,725.5 kcal/mol to 11,416.16 kcal/mol and stabilizes. The total system was converged in a straight line and we may consider that the system reached the equilibrium state.

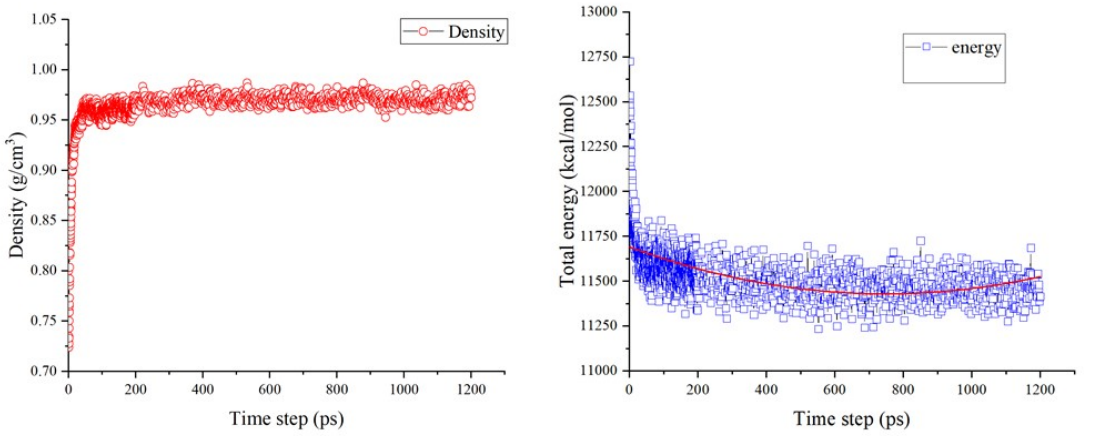

(a) Density of the bitumen model (b) Energy optimization of the bitumen model

Figure 4. Optimization of the bitumen model: (a) Density of the bitumen model; (b) Energy optimization of the bitumen model.

3.2. Polymer molecular models

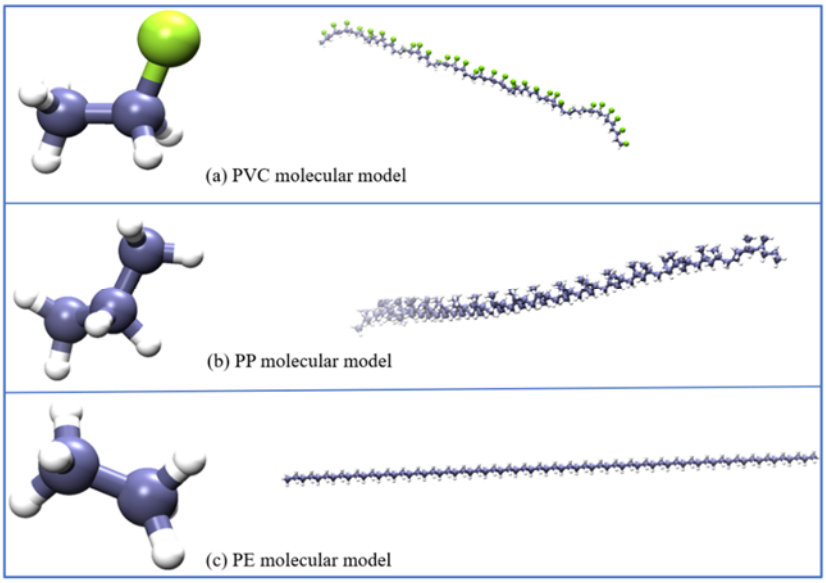

Figure 5. Polymer molecular models: (a) PVC molecular model; (b) PP molecular model; (c) PE molecular model (the carbon atom is purple, the hydrogen atom is white and the chlorine atom is green).

The construction of the molecular polymer model was based on its chemical formula first. In this study, the molecular formula of PVC is $(\mathrm{CH_2-CHCl})_n$, the molecular formula of PP is $(C_3H_6)_n$ and PE's molecular formula is $(CH_2-CH_2)_n$. These models need to be optimized because the initial energies of PVC, PP and PE are relatively high and the architectures are unstable. In this study, the repeat number of the PVC polymer was set to 35, that of the PP polymer to 40 and that of the PE polymer to 35 to construct the chain structure models of PVC, PP and PE, respectively. These molecular systems were optimized under the ACEFF, and the models are shown in Figure 5. The energies of models decreased, converged and stabilized with a certain number of iterations.

3.3. PVC-bitumen, PP-bitumen, and PE-bitumen blending models

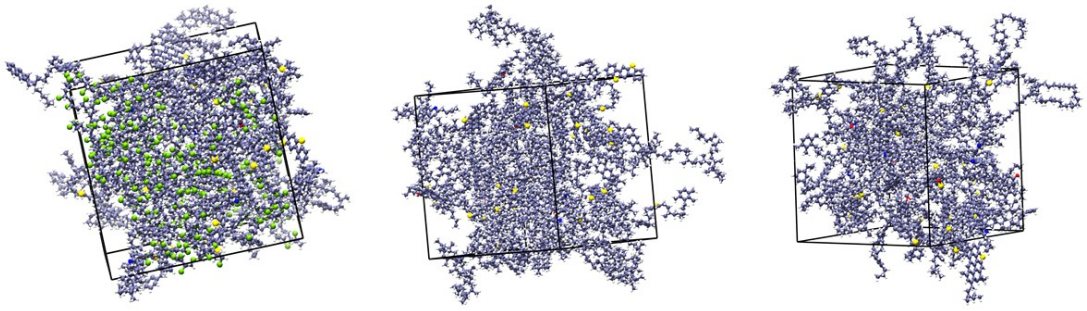

Figure 6. PVC-bitumen, PP-bitumen, and PE-bitumen blending models: (a) PVC-bitumen blending model; (b) PP-bitumen blending model; (c) PE-bitumen blending model (the carbon atom is purple, the oxygen atom is red, the nitrogen atom is blue, the sulfur atom is yellow, the chlorine atom is green and the hydrogen atom is white).

The blending systems (PVC-bitumen, PP-bitumen and PE-bitumen) were generated, respectively. The different energy optimization schemes and operations bring the blending systems to the equilibrium state. First, the system energy was optimized at a maximum of 5000 iterations by using the conjugate gradient method. Second, the system was subject to 100 atm and 298.15 K for 200 ps. Then, we ran the system for 1000 ps at 1 atm and 298.15 K. The blending models of PVC-bitumen, PP-bitumen and PE-bitumen are shown in Figure 6. These models were ready for the calculations of related properties.

4. Discussion on the compatibility of waste plastics and bitumen

The MD simulations were performed at 373.15, 393.15, 413.15, 433.1 and 453.15 K for the PVC, PP, PE, basic bitumen, PVC-bitumen blending system, PP- bitumen blending system and PE- bitumen blending system, which were constructed as described in Chapter 3. First, each system was applied under the NVT ensemble to be equilibrated at the target temperature, and the timestep was set at 500. Second, we ran 500 ps under the NVT ensemble to make the density of each system consistent with that of the real bitumen. Finally, the data with the most stable model density were selected for the parameter calculation and analysis. The calculation and analysis of solubility parameters and interaction energies were reliable under these simulation processes.

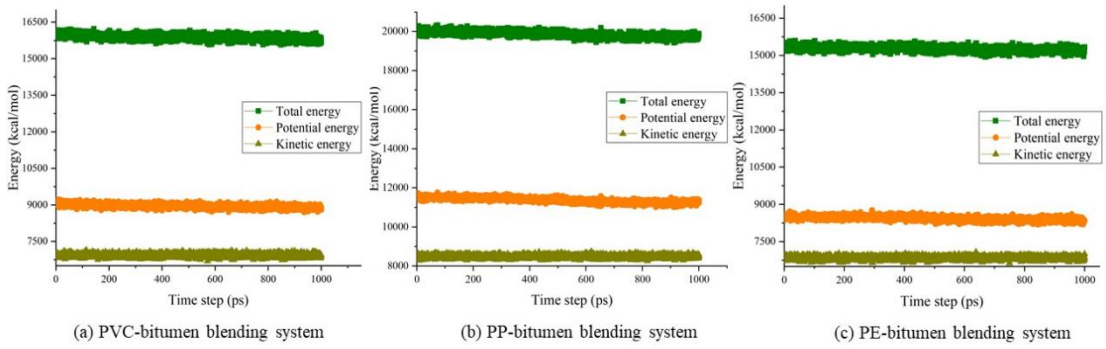

Figure7. Energy changes in different bitumen blending systems with different timesteps: (a) PVC-bitumen blending system; (b) PP-bitumen blending system; (c) PE-bitumen blending system.

All MD bitumen systems were simulated at different temperatures and conditions. Due to the intermolecular interactions, the bitumen systems were greatly changed internally during the simulations. The energy changes of the PVC-bitumen blending system, PP-bitumen blending system and PE-bitumen blending system are shown in Figure 7. It can be seen that the total energy, kinetic energy and potential energy converged gradually with the increase in simulation timesteps, which indicated stabilization of the structural energy of the system. Then, the solubility parameters and interaction energies were calculated as follows.

4.1. Solubility parameters

The compatibility can be characterized by a solubility parameter (δ). The blending effect is better when the parameter δ is close to each other. The solubility parameter δ can be obtained from the CED. The CED is defined as the cohesive energy per molecular system volume to separate all molecules to an infinite distance from each other, and its formula is given as Eq (2) [73]. The value of δ is the square root of the CED and it can be easily calculated from Eqs (3) and (4).

$$E_{coh} = -\langle E_{inter}\rangle = \langle E_{intra}\rangle = -\langle E_{total}\rangle \tag{2}$$

$$\mathrm{CED} = \frac{E_{coh}}{V} \tag{3}$$

$$\delta = \sqrt{CED} \tag{4}$$

where the symbol $\langle\ \ \rangle$ indicates an average over a canonical ensemble, E_{inter} is the energy between all molecules $(\mathrm{J/cm^3})$, E_{total} is the total energy of the molecular system $(\mathrm{J/cm^3})$, E_{intra} is the intra-molecular energy $(\mathrm{J/cm^3})$.

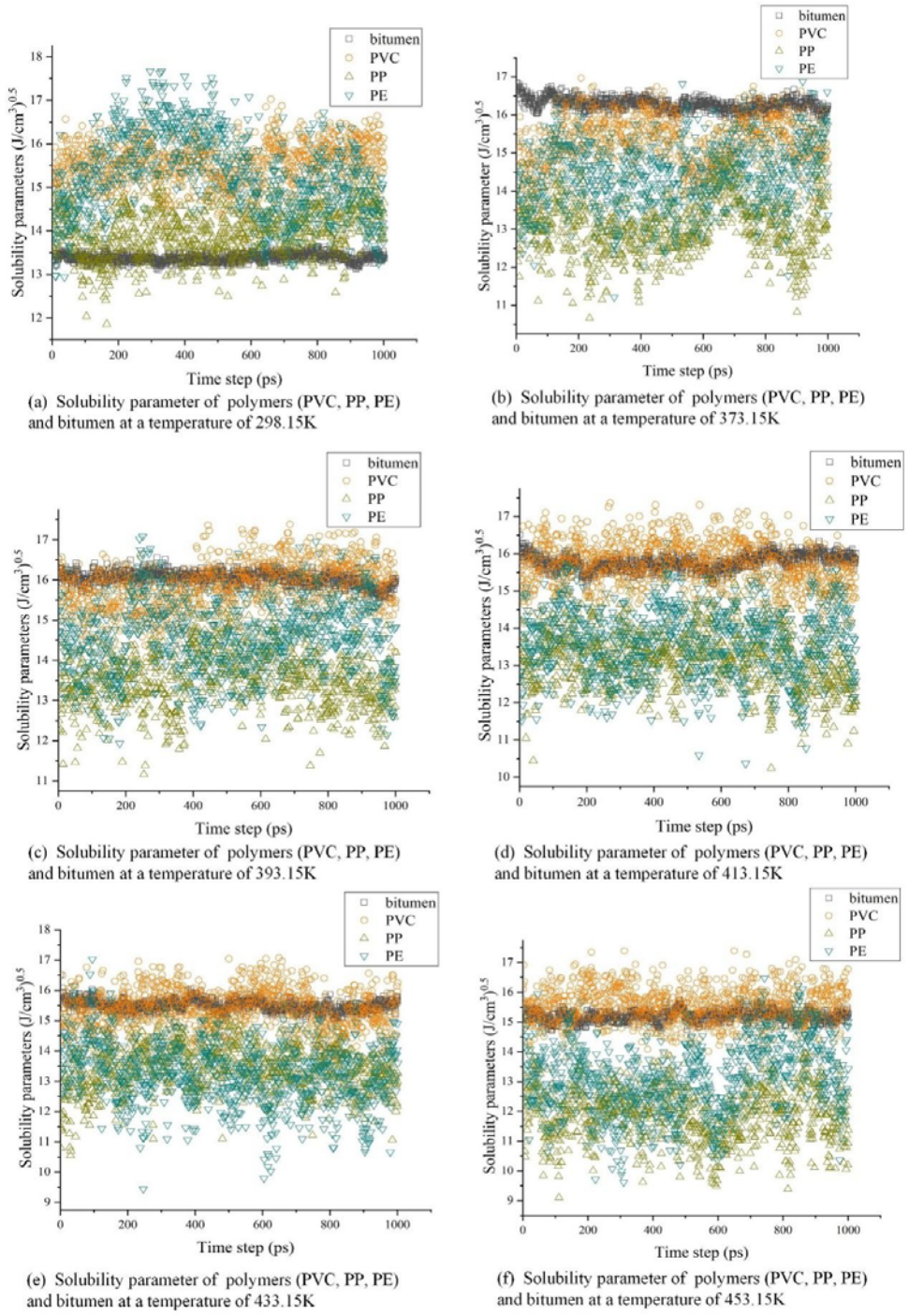

Figure 8. Solubility parameters for polymers (PVC, PP, PE) and bitumen, along with different simulation temperatures: (a) 298.15 K; (b) 373.15 K; (c) 393.15 K; (d) 413.15 K; (e) 433.15 K; (f) 453.15 K.

In the MD simulations, the CED is calculated to obtain the solubility parameter and thus evaluate the compatibility. When the difference between the solubility parameters of the two materials is in the range of 1.3–2.1 (J/cm^3), the two materials are compatible. The smaller the difference between the solubility parameters, the more the two are compatible. Therefore, in this study, the solubility parameter was chosen as an index to evaluate the compatibility degrees of PVC, PP and PE with bitumen, respectively.

Figure 8 shows the solubility parameters of the bitumen molecular system and polymer systems (PVC, PP and PE) at different temperatures. Figure 9(a) shows the solubility parameters of the systems at different temperatures after averaging. Obviously, the solubility parameter of bitumen shows a decreasing trend with the increase in the simulation temperature. However, the solubility parameters tend to increase at first for PVC, PP and PE polymers, followed by a decrease with the increase in temperature. In Figure 9(b), the difference between the solubility of bitumen and PVC and PP at 433.15 K is relatively smaller than that at other simulation temperatures. The difference for the PE system was also smaller at 393.15 K than that at other simulation temperatures. Therefore, it can be deduced that a better compatibility of bitumen with PVC and PP can be predicted and demonstrated at 433.15 K, and, also, better compatibility of bitumen with PE can be observed at 393.15 K. In addition, Figure 9(b) reflects that the difference in solubility between PP and bitumen is greater than that between PE and bitumen, and that the difference in solubility between PE and bitumen is larger than that between PVC and bitumen. It indicates that the compatibility degrees of PVC, PP and PE with bitumen may be ranked as PVC > PE > PP. In other words, among these three, the polymer PVC is the best option for compatibility with bitumen based on the simulation results. This indicates that additional processing is needed for PE and PP waste polymers when they are applied in pavement engineering.

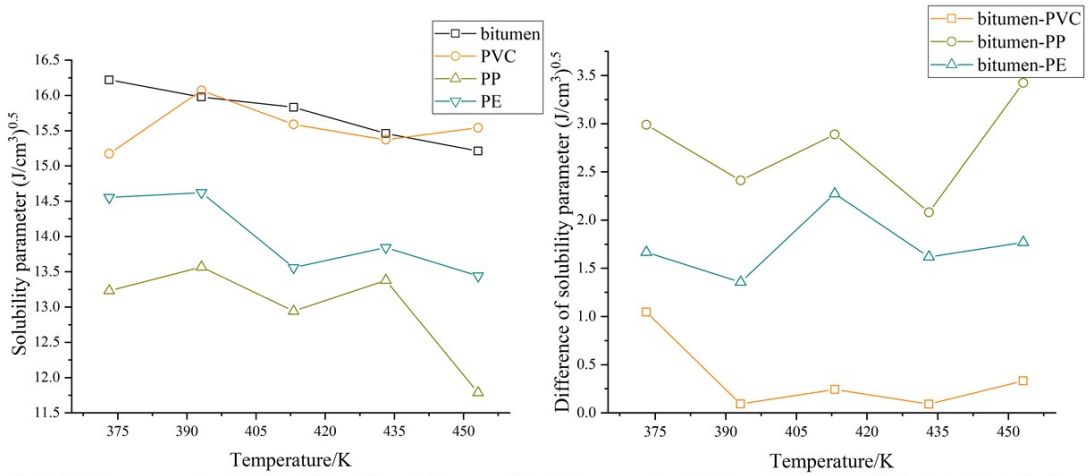

(a) Solubility parameter of PVC, PP, PE and bitumen (b) Difference of solubility parameter of PVC, PP, PE and bitumen

Figure 9. Changes in the average solubility of the polymers (PVC, PP, PE) and bitumen at different simulation temperatures: (a) Solubility of PVC, PP, PE and bitumen; (b) Difference in solubility of PVC, PP, PE and bitumen.

4.2. Interaction energy of the bitumen blending system

The interaction energy is influenced by the internal energy distribution and force fields used in different molecular systems when conducting the MD simulations. The non-bonding, van der Waals, and electrostatic energies were simulated and calculated to investigate the interaction energies of the polymers, bitumen and each blending system, respectively. The formulas used to calculate the different energies are given as Eqs (5)–(7).

$$E_{\text{int AB(no-bond)}} = E_{\text{AB(no-bond)}} - E_{\text{A(no-bond)}} - E_{\text{B(no-bond)}} \tag{5}$$

$$E_{\text{int AB(VDW)}} = E_{\text{AB(VDW)}} - E_{\text{A(VDW)}} - E_{B\text{(VDW)}} \tag{6}$$

$$E_{\text{int AB(e)}} = E_{\text{AB(e)}} - E_{\text{A(e)}} - E_{\text{B(e)}} \tag{7}$$

where $E_{\text{int AB(no-bond)}}$, $E_{\text{int AB(VDW)}}$ and $E_{\text{int AB(e)}}$ are the non-bonded, van der Waals, and electrostatic interaction energies between the A system and the B system, respectively. $E_{\text{AB(no-bond)}}$, $E_{\text{A(no-bond)}}$ and $E_{\text{B(no-bond)}}$ are the non-bonded energies of the A and B blending system and each A and B system, respectively. $E_{\text{AB(VDW)}}$, $E_{\text{A(VDW)}}$ and $E_{\text{A(VDW)}}$ are the van der Waals interaction energies of the A and B blending systems and each A and B system, respectively. $E_{\text{AB(e)}}$, $E_{\text{A(e)}}$ and $E_{\text{B(e)}}$ are electrostatic energies of the A and B blending systems, each A or B system, respectively.

The intermolecular interaction energy can be used to characterize the interaction strength and also predict the mixing ability and compatibility between two materials in one blended system. When the intermolecular interaction in the system is intense, the strong force observed maintains the high stability of the system. It is likely that good compatibility between materials can be deduced and inferred.

The van der Waals, electrostatic and non-bonded energies of all systems at different temperatures were calculated, and these are shown in Figure 10 according to Eqs (5)–(7). It can be seen that the electrostatic interactions of bitumen with PVC, PP and PE changed minimally for different simulation temperatures. However, the van der Waals and non-bonded energies fluctuated with an increase in temperature, and the two energies had the same trends with temperature. It may be inferred that the van der Waals energy makes a significant contribution to the non-bonded interaction and plays a dominant role in the miscibility of bitumen with PVC, PP and PE. The interaction energy between the bitumen and PVC molecules and PP molecules reached the maximum value at 433.15 K, and it reached the peak value at 393.15 K between the bitumen and PE molecules. It is possible that better compatibility between bitumen and PVC and PP molecules at 433.15 K, and also between bitumen and PE molecules at 393.15 K, can be predicted and deduced. Meanwhile, the ranking order of interaction energies between polymers and bitumen is PVC > PE > PP. The results are in agreement with those obtained from the analysis of the solubility parameters.

Figure 9 shows that the interaction energies of all systems were negative, indicating that the interaction between the bitumen and PVC molecules, PP molecules and PE molecules may be attractive in the polymer-bitumen blending systems. The interaction energies between the bitumen and PVC molecules and PP molecules were strongest at 433.15 K, and the interaction energy between the bitumen and PE molecules was strongest at 393.15 K. This indicates that as the temperature increases, the molecules in the blending systems move more vigorously. The interaction force between the molecules changes from repulsive to a gravitational force as the distance between the molecules increases. At 433.15 K, the gravitational force between PVC and bitumen (PP and bitumen) reached a maximum; at 393.15 K, the gravitational force between PE and bitumen reached a maximum. Therefore, the compatibility of the PVC-bitumen blending system and PP-bitumen blending system is the best at 433.15 K, and the compatibility of the PE-bitumen blending system is the best at 393.15 K, as compared to other temperatures.

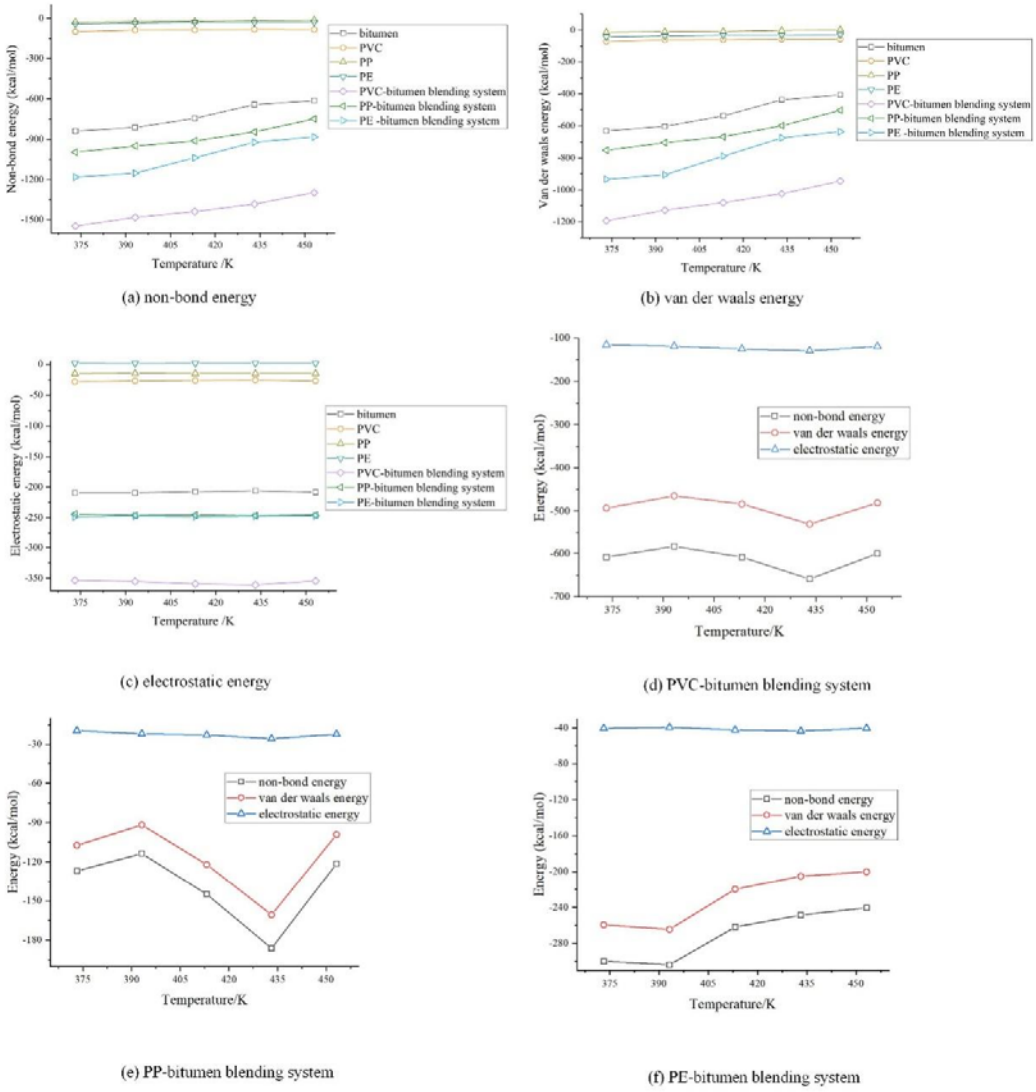

Figure 10. Energy changes in the polymers and each blending system according to simulation temperature: (a) Non-bonded energy; (b) van der Waals energy; (c) Electrostatic energy; (d) Energies in the PVC-bitumen blending system; (e) Energies in the PP-bitumen blending system; (f) Energies in the PE-bitumen blending system.

5. Conclusions

In this study, these molecular models were generated and established by MD methods focusing on bitumen, PVC, PP and PE. The compatibility analysis for waste polymers (PVC, PP and PE) and bitumen was investigated and explored for possible application in pavement engineering in large amounts. The solubility parameters and the interaction energies of different molecular systems were calculated and discussed to evaluate the compatibility of each of the polymers (PVC, PP and PE) with bitumen. The main conclusions are as follows:

1) The generation of polymer molecular models was based on the molecular structures of the polymers (PVC, PP and PE). The MD models of PVC-bitumen blending, PP-bitumen blending and PE-bitumen blending systems were based on the 12-molecule bitumen model and each polymer's

molecular model. The solubility of the bitumen and polymers (PVC, PP and PE) fluctuated with the increase in the simulation temperature. The solubility of bitumen exhibited a decreasing trend with increasing temperature, while the solubility values for the polymers (PVC, PP and PE) increase at the beginning, and then decrease with the increase in temperature. Compared to other temperatures, the $\Delta\delta$ between PVC and bitumen reached the minimum value at 433.15 K, indicating that the compatibility between PVC and bitumen may be better at this temperature. This was also the same situation for bitumen and polymer PP. Meanwhile, at the temperature of 393.15 K, the $\Delta\delta$ of PE and bitumen reached the minimum value, which means that PE and bitumen had a better miscible state at this temperature.

2) The energy results from the MD simulation show that van der Waals interaction and non-bonded interaction fluctuated with an increase in temperature. The van der Waals interaction played a dominant role in the compatibility between the bitumen and polymers (PVC, PP and PE). The electrostatic interaction fluctuates less with the increase in simulated temperature, while the van der Waals interaction and the non-bonded interaction fluctuate more. Moreover, the interaction energies between the bitumen and PVC and PP reached the maximum at 433.15 K, and the energies between bitumen and PE were maximum at 393.15 K. Therefore, it can be concluded that the compatibility of bitumen with PVC and PP is better at the temperature of 433.15 K, and that the compatibility of bitumen with the PE is also better at the temperature of 393.15 K compared to other temperatures.

3) A comparative analysis of the solubility and interaction energies was conducted and the results remained consistent. It can be deduced that certain blending condition combinations may yield better compatibility between the two materials, including PVC-bitumen at 433.15 K, PP-bitumen at 433.15 K and PE-bitumen at 393.15 K. Moreover, to a certain extent, the potential compatibility of PVC and bitumen may be better than that of the PE-bitumen and PP-bitumen combinations according to the simulation results for the solubility and interaction energies.

Therefore, waste polymers (PVC, PP and PE) can be used for the modification of bitumen, and they are largely applied in pavement engineering. In addition, this study analyzed the compatibility of polymers with bitumen only in terms of the state of the blending system; analyzing the adhesion between bitumen and polymers (PVC, PP and PE) by constructing interfacial models will be the next step in the study to understand the compatibility between bitumen and polymers.

Use of AI tools declaration

The authors declare they have not used artificial intelligence tools in the creation of this article.

Acknowledgments

The authors appreciate the financial support from Hunan Expressway Group Co. Ltd and the Hunan Department of Transportation (No. 202152) in China. The authors also appreciate the funding support from the Beijing high-level overseas talents and the National Science Foundation (USA) under grant no. 1300286. The MD simulation part in the project was conducted by using the LAMMPS (Large-scale Atomic/Molecular Massively Parallel Simulator) and MAPS Platform from Scienomics. All opinions, findings and conclusions expressed in this paper are those of the authors and do not necessarily represent the view of any organization.

Conflict of interest

The authors declare that there is no conflict of interest.

References

1. B. Madden, M. Jazbec, N. Florin, Increasing packaging grade recovery rates of plastic milk bottles in Australia: A material flow analysis approach, *Sustainable Prod. Consumption*, **37** (2023), 65–77. https://doi.org/10.1016/j.spc.2023.02.017
2. Y. Chen, Z. Cui, X. Cui, W. Liu, X. Wang, X. Li, et al., Life cycle assessment of end-of-life treatments of waste plastics in China, *Resour. Conserv. Recycl.*, **146** (2019), 348–357. https://doi.org/10.1016/j.resconrec.2019.03.011
3. W. Leal Filho, U. Saari, M. Fedoruk, A. Iital, H. Moora, M. Klöga, et al., An overview of the problems posed by plastic products and the role of extended producer responsibility in Europe, *J. Cleaner Prod.*, **214** (2019), 550–558. https://doi.org/10.1016/j.jclepro.2018.12.256
4. US EPA O, *Plastics: Material-Specific Data*, 2017. Available from: https://www.epa.gov/facts-and-figures-about-materials-waste-and-recycling/plastics-material-specific-data.
5. P. He, L. Chen, L. Shao, H. Zhang, F. Lü, Municipal solid waste (MSW) landfill: A source of microplastics? -Evidence of microplastics in landfill leachate, *Water Res.*, **159** (2019), 38–45. https://doi.org/10.1016/j.watres.2019.04.060
6. M. Sun, M. Zheng, G. Qu, K. Yuan, Y. Bi, J. Wang, Performance of polyurethane modified asphalt and its mixtures, *Constr. Build. Mater.*, **191** (2018), 386–397. https://doi.org/10.1016/j.conbuildmat.2018.10.025
7. P. J. Yoo, B. S. Ohm, J. Y. Choi, Toughening characteristics of plastic fiber-reinforced hot-mix asphalt mixtures, *KSCE J. Civ. Eng. Manage.*, **16** (2012), 751–758. https://doi.org/10.1007/s12205-012-1384-0
8. A. Behl, G. Sharma, G. Kumar, A sustainable approach: Utilization of waste PVC in asphalting of roads, *Constr. Build. Mater.*, **54** (2014), 113–117. https://doi.org/10.1016/j.conbuildmat.2013.12.050
9. Z. Leng, R. K. Padhan, A. Sreeram, Production of a sustainable paving material through chemical recycling of waste PET into crumb rubber modified asphalt, *J. Cleaner Prod.*, **180** (2018), 682–688. https://doi.org/10.1016/j.jclepro.2018.01.171
10. F. Sadiq Bhat, M. Shafi Mir, A study investigating the influence of nano Al_2O_3 on the performance of SBS modified asphalt binder, *Constr. Build. Mater.*, **271** (2021), 121499. https://doi.org/10.1016/j.conbuildmat.2020.121499
11. C. Yang, J. Xie, X. Zhou, Q. Liu, L. Pang, Performance evaluation and improving mechanisms of diatomite-modified asphalt mixture, *Materials*, **11** (2018), 686. https://doi.org/10.3390/ma11050686
12. M. Liang, S. Ren, C. Sun, J. Zhang, H. Jiang, Z. Yao, Extruded tire crumb-rubber recycled polyethylene melt blend as asphalt composite additive for enhancing the performance of binder, *J. Mater. Civ. Eng.*, **32** (2020), 04019373. https://doi.org/10.1061/(ASCE)MT.1943-5533.0003044
13. G. D. Airey, Rheological evaluation of ethylene vinyl acetate polymer modified bitumens, *Constr. Build. Mater.*, **16** (2002), 473–487. https://doi.org/10.1016/S0950-0618(02)00103-4

14. M. Bai, Investigation of low-temperature properties of recycling of aged SBS modified asphalt binder, *Constr. Build. Mater.*, **150** (2017), 766–773. https://doi.org/10.1016/j.conbuildmat.2017.05.206
15. R. K. Padhan, A. Sreeram, Enhancement of storage stability and rheological properties of polyethylene (PE) modified asphalt using cross linking and reactive polymer based additives, *Constr. Build. Mater.*, **188** (2018), 772–780. https://doi.org/10.1016/j.conbuildmat.2018.08.155
16. Z. Ren, Y. Zhu, Q. Wu, M. Zhu, F. Guo, H. Yu, et al., Enhanced storage stability of different polymer modified asphalt binders through nano-montmorillonite modification, *Nanomaterials*, **10** (2020), 641. https://doi.org/10.3390/nano10040641
17. D. Lo Presti, Recycled Tyre Rubber Modified Bitumens for road asphalt mixtures: A literature review, *Constr. Build. Mater.*, **49** (2013), 863–881. https://doi.org/10.1016/j.conbuildmat.2013.09.007
18. A. Topal, Evaluation of the properties and microstructure of plastomeric polymer modified bitumens, *Fuel Process. Technol.*, **91** (2010), 45–51. https://doi.org/10.1016/j.fuproc.2009.08.007
19. Y. Becker, M. Méndez, Y. Rodriguez, Polymer modified asphalt, *Vision Tecnol.*, **9** (2001), 39–50.
20. B. Sengoz, A. Topal, G. Isikyakar, Morphology and image analysis of polymer modified bitumens, *Constr. Build. Mater.*, **23** (2009), 1986–1992. https://doi.org/10.1016/j.conbuildmat.2008.08.020
21. C. Li, S. Fan, T. Xu, Method for evaluating compatibility between SBS modifier and asphalt matrix using molecular dynamics models, *J. Mater. Civ. Eng.*, **33** (2021), 04021207. https://doi.org/10.1061/(ASCE)MT.1943-5533.0003863
22. X. Yao, C. Li, T. Xu, Interfacial adhesive behaviors between SBS modified bitumen and aggregate using molecular dynamics simulation, *Surf. Interfaces*, **33** (2022), 102245. https://doi.org/10.1016/j.surfin.2022.102245
23. S. Wu, L. Montalvo, Repurposing waste plastics into cleaner asphalt pavement materials: A critical literature review, *J. Cleaner Prod.*, **280** (2021), 124355. https://doi.org/10.1016/j.jclepro.2020.124355
24. C. Vargas, A. El Hanandeh, Systematic literature review, meta-analysis and artificial neural network modelling of plastic waste addition to bitumen, *J. Cleaner Prod.*, **280** (2021), 124369. https://doi.org/10.1016/j.jclepro.2020.124369
25. P. J. Yoo, I. L. Al-Qadi, Pre- and post-peak toughening behaviours of fibre-reinforced hot mix asphalt mixtures, *Int. J. Pavement Eng.*, **15** (2014), 122–132. https://doi.org/10.1080/10298436.2013.839789
26. D. Movilla-Quesada, A. C. Raposeiras, L. T. Silva-Klein, P. Lastra-González, D. Castro-Fresno, Use of plastic scrap in asphalt mixtures added by dry method as a partial substitute for bitumen, *Waste Manage.*, **87** (2019), 751–760. https://doi.org/10.1016/j.wasman.2019.03.018
27. M. Arabani, M. Pedram, Laboratory investigation of rutting and fatigue in glassphalt containing waste plastic bottles, *Constr. Build. Mater.*, **116** (2016), 378–383. https://doi.org/10.1016/j.conbuildmat.2016.04.105
28. V. S. Punith, A. Veeraragavan, S. N. Amirkhanian, Evaluation of reclaimed polyethylene modified asphalt concrete mixtures, *Int. J. Pavement Res. Technol.*, **4** (2011), 1–10.
29. K. Pinsuwan, P. Opaprakasit, A. Petchsuk, L. Dubas, M. Opaprakasit, Chemical recycling of high-density polyethylene (HDPE) wastes by oxidative degradation to dicarboxylic acids and their use as value-added curing agents for acrylate-based materials, *Polym. Degrad. Stab.*, **210** (2023), 110306. https://doi.org/10.1016/j.polymdegradstab.2023.110306

30. S. Köfteci, P. Ahmedzade, B. Kultayev, Performance evaluation of bitumen modified by various types of waste plastics, *Constr. Build. Mater.*, **73** (2014), 592–602. https://doi.org/10.1016/j.conbuildmat.2014.09.067
31. M. Fakhri, E. Shahryari, T. Ahmadi, Investigate the use of recycled polyvinyl chloride (PVC) particles in improving the mechanical properties of stone mastic asphalt (SMA), *Constr. Build. Mater.*, **326** (2022), 126780. https://doi.org/10.1016/j.conbuildmat.2022.126780
32. U. Bagampadde, D. Kaddu, B. M. Kiggundu, Evaluation of rheology and moisture susceptibility of asphalt mixtures modified with low density polyethylene, *Int. J. Pavement Res. Technol.*, **6** (2013), 217–224.
33. Z. Du, C. Jiang, J. Yuan, F. Xiao, J. Wang, Low temperature performance characteristics of polyethylene modified asphalts—A review, *Constr. Build. Mater.*, **264** (2020), 120704. https://doi.org/10.1016/j.conbuildmat.2020.120704
34. S. Moubark, F. Khodary, A. Othman, Evaluation of mechanical properties for polypropylene modified asphalt concrete mixtures, *Int. J. Sci. Res. Manage.*, **5** (2017), 7797–7801. https://doi.org/10.18535/ijsrm/v5i12.28
35. E. Sembiring, H. Rahman, Y. M. Siswaya, Utilization of polypropylene to substitute bitumen for asphalt concrete wearing course (AC-WC), *Geomate J.*, **14** (2018), 97–102. https://doi.org/10.21660/2018.42.17347
36. C. Fang, L. Jiao, J. Hu, Q. Yu, D. Guo, X. Zhou, et al., Viscoelasticity of asphalt modified with packaging waste expended polystyrene, *J. Mater. Sci. Technol.*, **30** (2014), 939–943. https://doi.org/10.1016/j.jmst.2014.07.016
37. M. R. Mohd Hasan, B. Colbert, Z. You, A. Jamshidi, P. A. Heiden, M. O. Hamzah, A simple treatment of electronic-waste plastics to produce asphalt binder additives with improved properties, *Constr. Build. Mater.*, **110** (2016), 79–88. https://doi.org/10.1016/j.conbuildmat.2016.02.017
38. P. Lin, W. Huang, Y. Li, N. Tang, F. Xiao, Investigation of influence factors on low temperature properties of SBS modified asphalt, *Constr. Build. Mater.*, **154** (2017), 609–622. https://doi.org/10.1016/j.conbuildmat.2017.06.118
39. M. García-Morales, P. Partal, F. J. Navarro, C. Gallegos, Effect of waste polymer addition on the rheology of modified bitumen, *Fuel*, **85** (2006), 936–943. https://doi.org/10.1016/j.fuel.2005.09.015
40. V. O. Bulatović, V. Rek, K. J. Marković, Rheological properties and stability of ethylene vinyl acetate polymer-modified bitumen, *Polym. Eng. Sci.*, **53** (2013), 2276–2283. https://doi.org/10.1002/pen.23462
41. M. Singh, P. Kumar, M. R. Maurya, Effect of aggregate types on the performance of neat and EVA-modified asphalt mixtures, *Int. J. Pavement Eng.*, **15** (2014), 163–173. https://doi.org/10.1080/10298436.2013.812211
42. M. Á. Salas, H. Pérez-Acebo, V. Calderón, H, Gonzalo-Orden, Bitumen modified with recycled polyurethane foam for employment in hot mix asphalt, *Ing. Invest.*, **38** (2018), 60–66. https://doi.org/10.15446/ing.investig.v38n1.65631
43. M. Salas, H. Pérez-Acebo, Introduction of recycled polyurethane foam in mastic asphalt, *Gradevinar*, **70** (2018), 403–412. https://doi.org/10.14256/JCE.2181.2017

44. B. W. Colbert, Z. You, Properties of modified asphalt binders blended with electronic waste powders, *J. Mater. Civ. Eng.*, **24** (2012), 1261–1267. https://doi.org/10.1061/(ASCE)MT.1943-5533.0000504
45. B. W. Colbert, A. Diab, Z. You, Using M-E PDG to study the effectiveness of electronic waste materials modification on asphalt pavements design thickness, *Int. J. Pavement Res. Technol.*, **6** (2013), 319–326.
46. P. K. Singh, S. K. Suman, M. Kumar, Influence of recycled acrylonitrile butadiene styrene (ABS) on the physical, rheological and mechanical properties of bitumen binder, *Transp. Res. Procedia*, **48** (2020), 3668–3677. https://doi.org/10.1016/j.trpro.2020.08.081
47. J. Li, S. Jin, G. Lan, Z. Xu, L. Wang, N. Wang, Research on the glass transition temperature and mechanical properties of poly (vinyl chloride)/dioctyl phthalate (PVC/DOP) blends by molecular dynamics simulations, *Chin. J. Polym. Sci.*, **37** (2019), 834–840. https://doi.org/10.1007/s10118-019-2249-5
48. X. Guo, Y. Liu, J. Wang, Sorption of sulfamethazine onto different types of microplastics: A combined experimental and molecular dynamics simulation study, *Mar. Pollut. Bull.*, **145** (2019), 547–554. https://doi.org/10.1016/j.marpolbul.2019.06.063
49. A. I. Al-Hadidy, Engineering behavior of aged polypropylene-modified asphalt pavements, *Constr. Build. Mater.*, **191** (2018), 187–192. https://doi.org/10.1016/j.conbuildmat.2018.10.007
50. C. Yu, K. Hu, Y. Chen, W. Zhang, Y. Chen, R. Chang, Compatibility and high temperature performance of recycled polyethylene modified asphalt using molecular simulations, *Mol. Simul.*, **47** (2021), 1037–1049. https://doi.org/10.1080/08927022.2021.1944624
51. C. Yu, K. Hu, Q. Yang, D. Wang, W. Zhang, G. Chen, et al., Analysis of the storage stability property of carbon nanotube/recycled polyethylene-modified asphalt using molecular dynamics simulations, *Polymers*, **13** (2021), 1658. https://doi.org/10.3390/polym13101658
52. R. M. Izatt, S. R. Izatt, R. L. Bruening, N. E. Izatt, B. A. Moyer, Challenges to achievement of metal sustainability in our high-tech society, *Chem. Soc. Rev.*, **43** (2014), 2451–2475. https://doi.org/10.1039/C3CS60440C
53. B. J. Alder, T. E. Wainwright, Studies in molecular dynamics. I. General method, *J. Chem. Phys.* **31** (1959), 459–466. https://doi.org/10.1063/1.1730376
54. A. Rahman, Correlations in the motion of atoms in liquid argon, *Phys. Rev.*, **136** (1964), A405–A411. https://doi.org/10.1103/PhysRev.136.A405
55. H. Yao, J. Liu, M. Xu, J. Ji, Q. Dai, Z. You, Discussion on molecular dynamics (MD) simulations of the asphalt materials, *Adv. Colloid Interface Sci.*, **299** (2022), 102565. https://doi.org/10.1016/j.cis.2021.102565
56. F. Khabaz, R. Khare, Glass transition and molecular mobility in styrene-butadiene rubber modified asphalt, *J. Phys. Chem. B*, **119** (2015), 14261–14269. https://doi.org/10.1021/acs.jpcb.5b06191
57. P. W. Jennings, J. A. Pribanic, M. A. Desando, M. F. Raub, R. Moats, J. A. Smith, et al., *Binder Characterization and Evaluation by Nuclear Magnetic Resonance Spectroscopy*, 1993, Washington, DC.
58. A. T. Pauli, F. P. Miknis, A. G. Beemer, J. J. Miller, Assessment of physical property prediction based on asphalt average molecular structures, *Preprints-American Chemical Society. Division of Petroleum Chemistry*, **50** (2005), 255–259.

59. L. W. Corbett, Composition of asphalt based on generic fractionation, using solvent deasphaltening, elution-adsorption chromatography, and densimetric characterization, *Anal. Chem.*, **41** (1969), 576–579. https://doi.org/10.1021/ac60273a004
60. L. Zhang, M. L. Greenfield, Analyzing properties of model asphalts using molecular simulation, *Energy Fuels*, **21** (2007), 1712–1716. https://doi.org/10.1021/ef060658j
61. L. Artok, Y. Su, Y. Hirose, M. Hosokawa, S. Murata, M. Nomura, Structure and reactivity of petroleum-derived asphaltene, *Energy Fuels*, **13** (1999), 287–296. https://doi.org/10.1021/ef980216a
62. D. D. Li, M. L. Greenfield, Chemical compositions of improved model asphalt systems for molecular simulations, *Fuel*, **115** (2014), 347–356. https://doi.org/10.1016/j.fuel.2013.07.012
63. S. Ren, X. Liu, P. Lin, Y. Gao, S. Erkens, Insight into the compatibility behaviors between various rejuvenators and aged bitumen: Molecular dynamics simulation and experimental validation, *Mater. Des.*, **223** (2022), 111141. https://doi.org/10.1016/j.matdes.2022.111141
64. X. Xin, Z. Yao, J. Shi, M. Liang, H. Jiang, J. Zhang, et al., Rheological properties, microstructure and aging resistance of asphalt modified with CNTs/PE composites, *Constr. Build. Mater.*, **262** (2020), 120100. https://doi.org/10.1016/j.conbuildmat.2020.120100
65. M. N. Rahman, M. Ahmeduzzaman, M. A. Sobhan, T. U. Ahmed, Performance evaluation of waste polyethylene and PVC on hot asphalt mixtures, *Am. J. Civil Eng. Archit.*, **1** (2013), 97–102. https://doi.org/10.12691/ajcea-1-5-2
66. S. Tapkın, The effect of polypropylene fibers on asphalt performance, *Build. Environ.*, **43** (2008), 1065–1071. https://doi.org/10.1016/j.buildenv.2007.02.011
67. M. Su, J. Zhou, J. Lu, W. Che, H. Zhang, Using molecular dynamics and experiments to investigate the morphology and micro-structure of SBS modified asphalt binder, *Mater. Today Commun.*, **30** (2022), 103082. https://doi.org/10.1016/j.mtcomm.2021.103082
68. F. Guo, J. Zhang, J. Pei, W. Ma, Z. Hu, Y. Guan, Evaluation of the compatibility between rubber and asphalt based on molecular dynamics simulation, *Front. Struct. Civ. Eng.*, **14** (2020), 435–445. https://doi.org/10.1007/s11709-019-0603-x
69. M. Liang, X. Xin, W. Fan, J. Zhang, H. Jiang, Z. Yao, Comparison of rheological properties and compatibility of asphalt modified with various polyethylene, *Int. J. Pavement Eng.*, **22** (2021), 11–20. https://doi.org/10.1080/10298436.2019.1575968
70. W. D. Cornell, P. Cieplak, C. I. Bayly, I. R. Gould, K. M. Merz, D. M. Ferguson, et al., A second generation force field for the simulation of proteins, nucleic acids, and organic molecules J. Am. Chem. Soc. 1995, 117, 5179−5197, *J. Am. Chem. Soc.*, **118** (1996), 2309–2309. https://doi.org/10.1021/ja955032e
71. M. Valiev, E. J. Bylaska, N. Govind, K. Kowalski, T. P. Straatsma, H. J. J. Van Dam, et al., NWChem: A comprehensive and scalable open-source solution for large scale molecular simulations, *Comput. Phys. Commun.*, **181** (2010), 1477–1489. https://doi.org/10.1016/j.cpc.2010.04.018
72. H. Yao, J. Liu, M. Xu, A. Bick, Q. Xu, J. Zhang, Generation and properties of the new asphalt binder model using molecular dynamics (MD), *Sci. Rep.*, **11** (2021), 9890. https://doi.org/10.1038/s41598-021-89339-5

73. X. Yu, J. Wang, J. Si, J. Mei, G. Ding, J. Li, Research on compatibility mechanism of biobased cold-mixed epoxy asphalt binder, *Constr. Build. Mater.*, **250** (2020), 118868. https://doi.org/10.1016/j.conbuildmat.2020.118868

AIMS Press